High-statistics investigation of K^0K^- decay of A_2^- produced by 23-GeV/c π^- on hydrogen

M. Margulies* and M. A. Kramer
City College of New York, New York, New York 10031†

K. J. Foley, W. A. Love, S. Ozaki, E. D. Platner, A. C. Saulys, and E. H. Willen
Brookhaven National Laboratory, Upton, New York 11973‡

S. J. Lindenbaum
Brookhaven National Laboratory, Upton, New York 11973‡
and City College of New York, New York, New York 10031†
(Received 29 April 1976)

We present the results of an experiment to study the reaction $\pi^-p \to A_2^-p$, $A_2^- \to K_S^0K^-$ at 22.4 and 23.9 GeV/c. We have 3346 $K_S^0K^-$ events in the effective mass region 1.1 to 1.5 GeV, and covering the $|t'|$ interval 0.0 to 1.0 (GeV/c)^2. Because of the low background in this channel, we are able to study various $|t'|$ regions, including the region 0.2 to 0.29 (GeV/c)^2 in which the original split A_2 peak was observed. We find no substructure in any region. We have also derived differential and total cross sections. The differential cross sections are well fitted by the form $d\sigma/dt' = At'e^{bt'}$ with $b \approx 7.0$ (GeV/c)$^{-2}$. The total cross section is in good agreement with the value derived from other experiments that measure the $A_2^- \to \rho^0\pi^-$ decay mode.

I. INTRODUCTION

We have studied the reaction $\pi^-p \to K_S^0K^-p$ at incident-pion momenta of 22.4 and 23.9 GeV/c. The experiment was performed using the Brookhaven National Laboratory (BNL) Mark I spectrometer. The primary aim of the experiment was to study the detailed structure of the A_2 mass spectrum. We have also measured differential and total cross sections.

The announcement of structure in the A_2 meson found with the CERN missing-mass spectrometer[1] (MMS) and its subsequent confirmation by use of the CERN boson spectrometer (CBS) in both an essentially missing-mass experiment[2] and an experiment that studied the $K_S^0K^-$ decay mode[3] generated a great deal of excitement and many attempts to confirm that result. A subsequent high-statistics bubble-chamber experiment[4] had about 1300 A_2^+ events, primarily in the 3π channel, and showed no evidence for a split.

At this point numerous experiments were underway to investigate the splitting either by using the missing-mass technique or by studying the A_2 decay in a channel with low background such as K^-K^0 or $\eta^0\pi^-$.

Two experiments[5,6] on the mode $A_2^- \to K_S^0K^-$ were reported, both of which rejected the splitting for the A_2 when integrated over the t' bite $0<|t'|<0.8$ (GeV/c)^2 but did not have sufficient statistics to make a definitive statement in the exact t' region [$0.2<|t'|<0.29$ (GeV/c)^2] investigated in the original CERN experiment[1] ($t' = t - t_{\min}$, where t is the negative square of the four-momentum transfer). Then missing-mass experiments[7,8] with setups similar to and with resolutions and statistics equivalent to or better than the original MMS and CBS also produced results that contradicted the original reports.

In the missing-mass experiments the signal-to-noise ratio at the A_2 region is of the order of 1:3 to 1:5, allowing for some controversy over the treatment of background in the contradictory experiments. In addition, the determination of the resolution involved some indirect arguments. Thus, it was still conceivable that the splitting of the A_2 could be t' dependent.

The present experiment has high statistics in the $K_S^0K^-$ channel where the background is low. We studied the A_2^- mass spectrum in the t' regions $0<|t'|<0.2$, $0.2<|t'|<0.29$, and $|t'|>0.29$ (GeV/c)^2, and thus could test the possibility that the A_2^- mass spectrum is t' dependent in such a way as to cause a split in the t' region studied by the CERN MMS or in other t' regions.

There was also some special interest in the cross sections, since at the time of the 1972 XVI International Conference on High Energy Physics it appeared that there might be a discrepancy between the energy dependence of the A_2 cross section as determined from the $\rho\pi$ and $\bar{K}K$ decay modes.[9]

Preliminary data from this experiment were reported at the XVII International Conference on High Energy Physics.[10]

II. EXPERIMENTAL ARRANGEMENT AND PROCEDURE

The experiment was run at the Brookhaven AGS using the forward arm of the BNL Mark I spectrometer shown in Fig. 1. It was a high-resolution magnetic spectrometer with magnetostrictive-readout spark chambers in front of and behind a large-aperture bending magnet (48D48).

The topology of the desired $K^0_S K^-$ events was characterized by a single charged particle (the K^-) leaving the interaction and a vee resulting from the decay of the K^0_S into a pair of charged pions. The pulse height of the signal from scintillator A was used to determine that one and only one charged particle had emerged from the target. The multiwire proportional counter (PWC) and hodoscopes $H4$ and $H4'$ were used to determine that there were three tracks downstream of spark chamber A.

The beam and detection apparatus were essentially the same as those for the experiment published earlier (experiment I).[5,11] The momentum of the beam was raised from 20.3 GeV/c to 22.4 GeV/c for part of this run and to 23.9 GeV/c for the remainder. The beam intensity was raised to 10^5 particles per spill in a pulse 750 msec long.

In order to increase the acceptance, the apparatus of experiment I was rearranged as follows. The distance from the H_2 target to the 48D48 analyzing magnet was reduced from 470 cm to 300 cm by removing one of the B spark-chamber modules and reducing the distance between the H_2 target and the first (A) spark-chamber module from 170 cm to 65 cm. The resolution of the three-particle trigger device was improved by replacing the scintillation-counter hodoscope $H6$ with a multiwire proportional counter. A small scintillator, B ($13\times13\times0.3$ cm), was added behind $H4'$ and used to veto beam particles which had not interacted in the hydrogen target. The front face and the interior sides of the 48D48 magnet were also lined with veto scintillators to reject events where one or more particles struck the magnet steel. The resultant trigger rate was one in 20 000 incident beam particles as compared to one in 5000 in experiment I.

The off-line analysis was performed on the BNL CDC 6600 computers. Sparks were combined into straight-line tracks in the X and Y "views" separately. These tracks were associated into three-dimension tracks by using the sparks in the w view (oriented at 45°). The track segments were then connected through the magnet. Events containing both a negative track and one neutral vee whose effective mass was between 0.485 and 0.510 GeV were considered to be $K^0_S K^-$ candidates and were written on a summary tape. The yield of such events was 3.1% of all triggers in this experiment as compared to 0.5% in experiment I.

Since the decay products were not identified in the spectrometer, the above sample included both $K^0_S K^-$ and $K^0_S \pi^-$ events. The effective-mass distribution for these events, assuming the negative particle is a K^-, is shown in Fig. 2. No correction has been applied for the acceptance of the apparatus. A bump on top of a rather large background can be seen in the region of 1.3 GeV. The missing-mass spectrum of the events for the K^0K^- hypothesis is shown in Fig. 3. There is a clear peak at the proton mass with a $\sigma_{\rm rms}$ of ~80 MeV. We selected the events with a missing mass in the region of 0.7 to 1.1 GeV. We note that this cut also removed the $K^0_S\pi^-$ events from our resulting data sample. Strangeness and baryon conservation for a $\pi^- p \to K^0_S \pi^- X^+$ event would require a recoil mass at least as large as that of a Σ^+. Calculating the recoil missing mass for such an event on the $K^0_S K^-$ hypothesis would only lower the true mass by $\lesssim 20$ MeV; thus, it would be removed by the above cut. The final sample of $K^0_S K^-$ events selected on the basis of the recoil-proton mass is shown in Fig. 4(a).

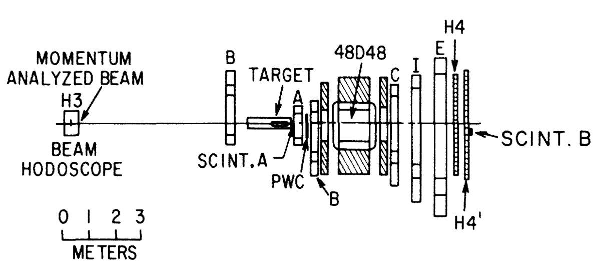

FIG. 1. The forward arm of the BNL Mark I spectrometer. The symbols A, B, C, I, and E identify spark chambers. Scint. A and Scint. B are scintillation counters. $H4$ and $H4'$ are scintillation-counter hodoscopes.

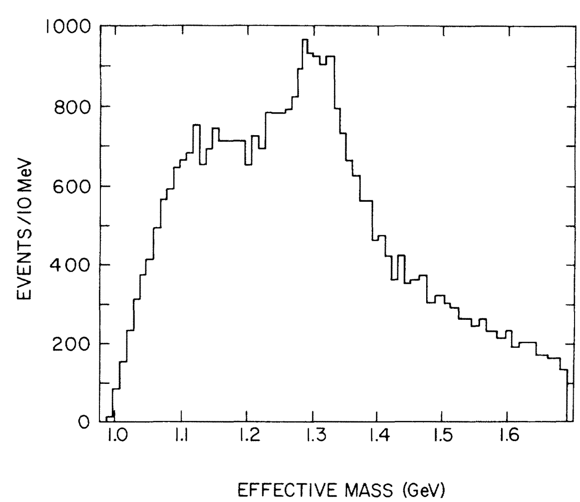

FIG. 2. The effective mass for all events containing a K^0_S and a negative track analyzed as $K^0_S K^-$ events.

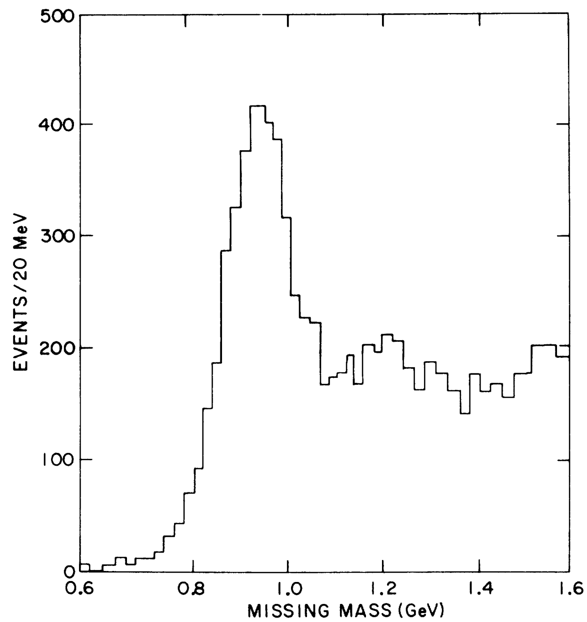

FIG. 3. The missing-mass spectrum for all the events containing a K_s^0 and a negative track analyzed as $K_s^0K^-$ events.

III. MASS RESOLUTION

The angular resolution of the forward arm of the spectrometer was determined from beam tracks that traversed the entire system with the spectrometer magnet off. The difference between the angle of the track as measured by the upstream and downstream arms of the spectrometer was calculated and an rms deviation was obtained for that distribution. The contributions of the upstream and downstream arms were then unfolded to yield the rms angular resolution for each. The projected angular resolution in the horizontal plane of the upstream arm as a function of momentum is shown in Fig. 5.

The momentum resolution was determined by triggering on beam tracks with the magnet on. The difference between the momentum of a track as calculated by the incident-beam spectrometer and as calculated by the Mark I spectrometer was plotted and an rms deviation was obtained for this distribution. We then unfolded the resolution of the beam spectrometer to determine the momentum resolution of the Mark I spectrometer. Figure 6 is a plot of this resolution as a function of

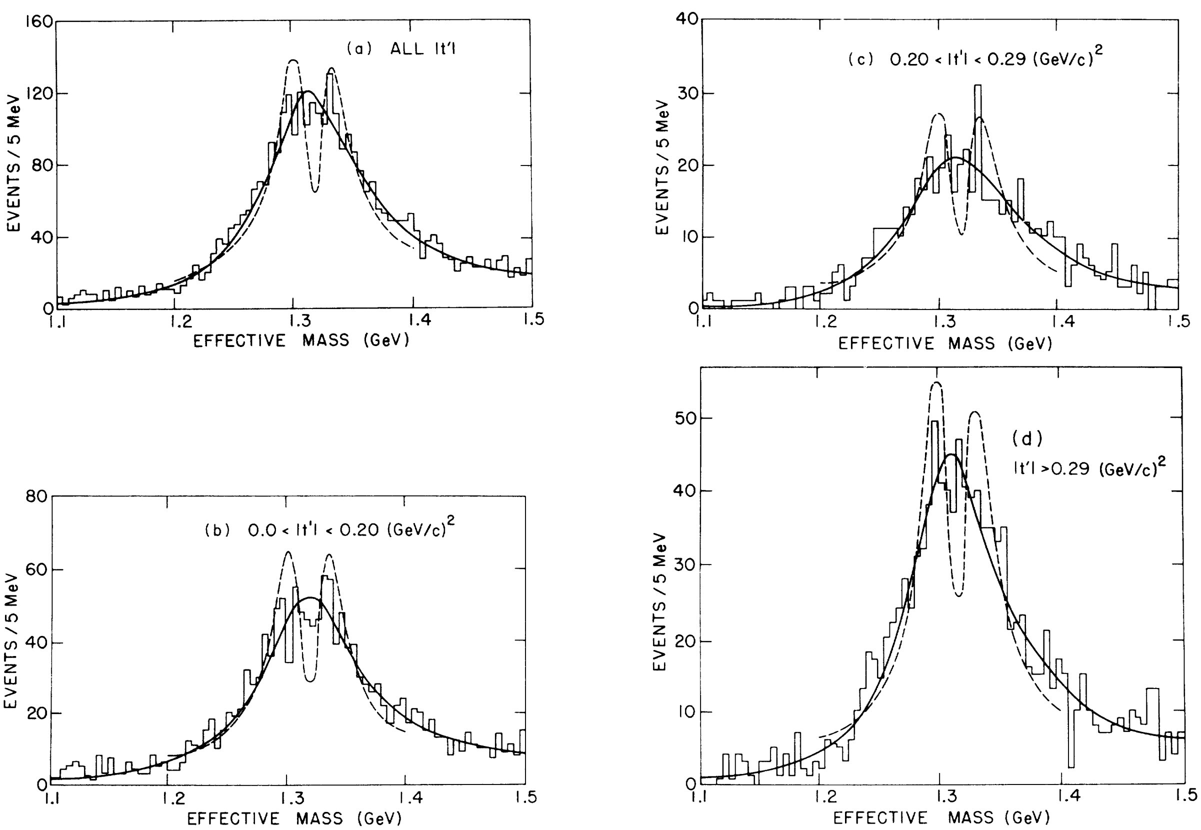

FIG. 4. The $K_s^0K^-$ mass spectrum for those events having a missing mass between 0.7 and 1.1 GeV/c. The solid curves represent the fit by a D-wave Breit-Wigner form plus a linear background. The dashed curves represent the best fits to a dipole form plus a linear background. For (b), (c), and (d), the background level was obtained from a similar fit over the region $1.1 < M(K_s^0K^-) < 1.7$ GeV (see text). (a) all t', (b) $|t'| < 0.2$, (c) $0.20 < |t'| < 0.29$, and (d) 0.29 $(\text{GeV}/c)^2 < |t'|$.

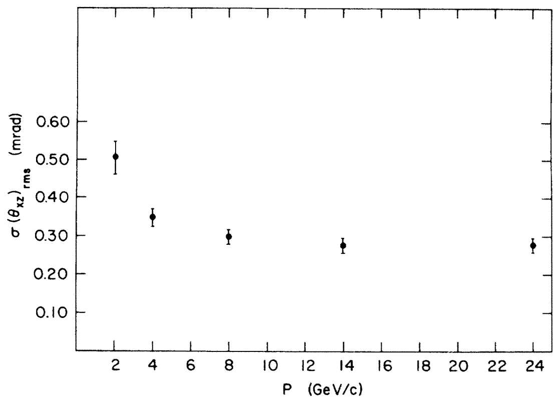

FIG. 5. The angular resolution in the horizontal projection of the upstream arm of the spectrometer plotted as a function of momentum.

momentum.

We checked our resolution determinations by calculating the expected K_S^0 mass resolution and comparing it to the experimentally observed mass spectrum of K_S^0's from the A_2 decay. The observed K_S^0's have momenta that vary over the range of 3.5 to 19.5 GeV/c, and the decay pions have momenta that range from 1.5 to 17 GeV/c, peaking at 5 GeV/c. We used the momentum-dependent angular and momentum resolutions determined above to calculate an expected mass resolution for each event in our data and then evaluated the mean effective mass resolution for all K_S^0's. The result was

$$\sigma(M_{K_S^0})=2.9\pm0.3 \text{ MeV (calculated)},$$

in good agreement with the value

$$\sigma(M_{K_S^0})=3.0\pm0.1 \text{ MeV}$$

(experimental—single Gaussian)

derived from fitting the observed experimental distribution to the form of a Gaussian plus a linear background. The background given by this fit is 10% of the total $\pi^+\pi^-$ events in the range $0.485 < M(\pi^+\pi^-) < 0.510$ MeV. However, this form (shown as the dashed curve in Fig. 7) has difficulty fitting both the peak and the tails and thus may be slightly underestimating the tails of the distributions. To evaluate this possibility, we fitted the $\pi^+\pi^-$ mass spectrum to a form consisting of the sum of two Gaussian terms and a linear background. This gave a good fit [$\chi^2=49.9$ for 44 degrees of freedom (DOF)] with the values of $\sigma_1=2.2$ MeV and $\sigma_2=4.3$ MeV for the widths of the two Gaussians. This fit is plotted as the solid curve on Fig. 7. The wider Gaussian has an amplitude that is $(58\pm18)\%$ of the narrower one. The fitted background is 5%. The rms width for the sum of the two Gaussians is

$$\sigma(M_{K_S^0})=3.5\pm0.35 \text{ MeV}$$

(experimental—two Gaussians).

Thus we estimate the effect of the tails of the resolution functions to be less than or of the order of 17%

The best-fit value of the K^0 mass given by the above fits was 497.3 ± 0.3 MeV. We estimate the systematic error in this mass to be about 0.5 MeV.

The A_2 effective-mass resolution was derived by using the momentum-dependent angular and momentum resolution functions and calculating the expected σ for each of our events. Additional

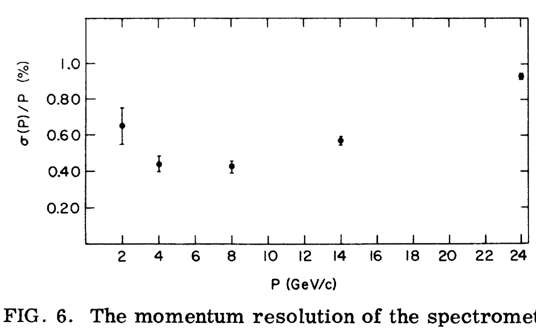

FIG. 6. The momentum resolution of the spectrometer as a function of momentum.

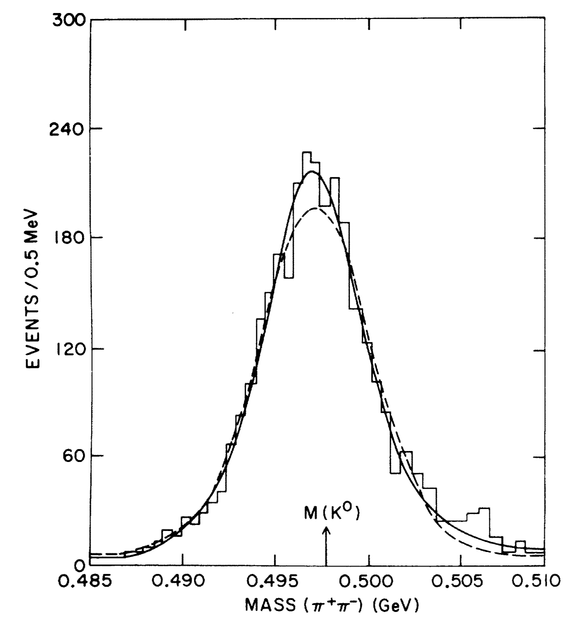

FIG. 7. The $\pi^+\pi^-$ effective-mass distribution in the region of the K^0 for $K_S^0K^-$ events with effective masses between 1.1 and 1.5 GeV. The dashed curve represents a fit to this spectrum using a single Gaussian and a linear background. The solid curve represents a fit using two Gaussians with different widths plus a linear background.

multiple scattering was included for the K^- as a function of the decay point of the A_2^- to account for its scattering in the liquid hydrogen, the target walls, and the scintillator A. Averaging over all events, this gave us a mean value of

$$\sigma(M_{A_2^-}) = 4.25 \pm 0.4 \text{ MeV}.$$

In order to be conservative and to allow for the possible effects of the tails of the distributions as observed previously for the K_S^0, we used the value of

$$\sigma(M_{A_2^-}) = 5 \text{ MeV}$$

in all of the subsequent fits to the A_2^- mass spectra.

IV. MASS SPECTRUM

The $K_S^0K^-$ effective-mass spectrum between 1.1 and 1.5 GeV for those events with a missing mass between 0.7 and 1.1 GeV (i.e., proton recoil) is shown in Fig. 4(a). There are 3346 events in this spectrum (2370 at 23.9 GeV/c and 976 at 22.4 GeV/c). The spectrum is not corrected for the acceptance of the spectrometer, which varies by less than 20% from 1.2 to 1.4 GeV as shown in Fig. 8.

There is no statistically significant structure within the A_2 peak. We have performed a maximum-likelihood fit to the data with a D-wave Breit-Wigner form and a linear background starting at threshold. In fitting the data we have folded in a mass resolution of 5 MeV and multiplied the theoretically expected distribution by the acceptance of the spectrometer. The Breit-Wigner form used was as follows[12]:

$$N(M) = \frac{MM_0\Gamma(M)}{(M^2 - M_0^2)^2 + [M_0\Gamma(M)]^2}$$

and

$$\Gamma(M) = \Gamma_0 \left(\frac{q}{q_0}\right)^5 \frac{\rho(q)}{\rho(q_0)} ,$$

where $q_0 = q(M_0)$ and q is the momentum of either the K^0 or the K^- in the A_2 rest frame. $\rho(q)$ is a slowly varying factor correcting for angular-momentum-barrier effects. We have used

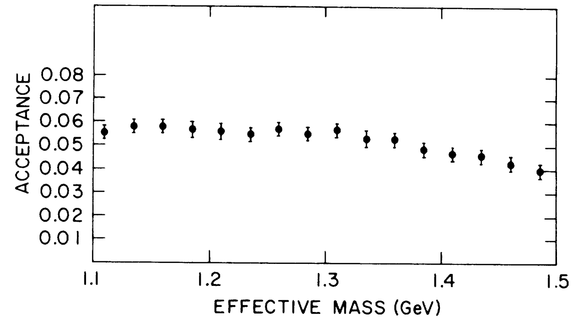

FIG. 8. The acceptance of the spectrometer as a function of effective mass at 23.9 GeV/c.

$$\rho(q) = (9 + 3R^2q^2 + R^4q^4)^{-1} ,$$

where R is fitted as a free parameter. The results of a maximum-likelihood fit to the overall $K_S^0K^-$ effective-mass spectrum in the mass region 1.1–1.5 GeV are $m_0 = 1.320 \pm 0.002$ GeV, $\Gamma_0 = 0.105 \pm 0.006$ GeV, $R = 4.4 \pm 0.7$ GeV^{-1}, and $\chi^2 = 69$ for 76 degrees of freedom.

We also fitted the data with the above D-wave Breit-Wigner form and a linear background starting at threshold, for the following t' intervals:

$$0.0 < |t'| < 0.2 \ (\text{GeV}/c)^2 ,$$

$$0.2 < |t'| < 0.29 \ (\text{GeV}/c)^2 ,$$

and

$$0.29 \ (\text{GeV}/c)^2 < |t'| .$$

The results of these fits in the mass interval 1.1–1.5 GeV are given in Table I (fits 1–4) and are shown as the solid curves in Figs. 4(a)–4(d). For all of the fits listed in Table I, we have allowed the mass, the width, R, and the slope of the background to be free parameters. The stated errors are statistical only. We estimate that the mass scale is uncertain by ≈ 1 MeV.

We conclude that a single D-wave Breit-Wigner form of the same width and mean mass (plus a

TABLE I. Results of D-wave Breit-Wigner fits to the K^0K^- mass spectra from 1.1 to 1.5 GeV. The errors shown are statistical only.

Fit no.	$-t'$ [(GeV/c)^2]	M_0 (GeV)	Γ_0 (GeV)	R (GeV^{-1})	χ^2	Degrees of freedom	Total events	Fitted background
(1)	All t'	1.320 ± 0.002	0.105 ± 0.006	4.4 ± 0.7	69	76	3346	622
(2)	0.0–0.2	1.320 ± 0.002	0.094 ± 0.008	8.7 ± 4.3	63	76	1539	370
(3)	0.2–0.29	1.323 ± 0.004	0.122 ± 0.014	4.5 ± 1.4	53	76	633	63
(4)	>0.29	1.319 ± 0.003	0.105 ± 0.010	2.8 ± 1.0	81	76	1174	161

background level ~10–20%) fits the data very well (χ^2 per degree of freedom ≈ 1) in all t' intervals investigated.

We have also attempted to fit the data with the following dipole shape used in the analysis of the CERN missing-mass data:

$$N(M)=\frac{\Gamma^2(M-M_0)^2}{[(M-M_0)^2+\frac{1}{4}\Gamma^2]^2}\ ,$$

using 5 MeV for the mass resolution and allowing Γ, M_0, and the slope of the background to be free parameters. The dashed curve on Fig. 4(a) is the best fit to the overall mass spectrum for $1.1 < M(K_S^0K^-) < 1.5$ GeV, using the above dipole form and a linear background starting at threshold. The best fit has a χ^2 of 205 for 77 degrees of freedom, which corresponds to a rejection of 8 standard deviations. [See Table II, fit (1).]

In order to concentrate on the region where the functional form has a dip and to eliminate contributions to the χ^2 from the tails of the mass spectrum, we also fitted the total data sample in the mass region $1.25 < M(K_S^0K^-) < 1.35$ GeV (see Fig. 9). The background level was fixed at that determined by a dipole fit over the mass range $1.1 < M(K_S^0K^-) < 1.5$ GeV (the background was 24% of the total events and less than 15% of the peak height). The best fit has a χ^2 of 71 for 17 DOF or a 6-standard-deviation rejection. [See Table II, fit (5).]

The data were then broken into different t' intervals as for the Breit-Wigner fits above. Each set was then fitted to a dipole plus a linear background in the mass range $1.2 < M(K_S^0K^-) < 1.4$ GeV. Since this mass range is too narrow to reasonably determine the true background level, we first fitted each spectrum to a dipole plus a linear background over the range $1.1 < M(K_S^0K^-) < 1.7$ GeV. The background level so obtained (≈ 19% of the total events) was then used as a fixed background for a fit in the mass interval $1.2 < M(K_S^0K^-) < 1.4$ GeV, in which M_0 and Γ were free parameters. The dashed curves in Figs. 4(b) – 4(d) show the best fits to the mass spectra in the above mass range (1.2–1.4 GeV) for the t' intervals $|t'| < 0.20$, $0.20 < |t'| < 0.29$, and $|t'| > 0.29$ (GeV/c)^2, respectively. The probability for the fits in these t' intervals corresponded to 3.1σ, 2.6σ, and 3.9σ respectively. Table II gives the details of the fits to the CERN dipole form for the three t' intervals mentioned above. A similar fit to the total spectra yielded a χ^2 of 164 for 37 DOF corresponding to a rejection of 9.6σ.

V. DIFFERENTIAL AND TOTAL CROSS SECTIONS

The data were divided into t' intervals, and the mass spectrum corresponding to each interval was fitted to a form consisting of a D-wave Breit-Wigner form plus a linear background starting at threshold. The parameters of the A_2 were fixed at values obtained from the fit to the overall spectrum ($M_0 = 1.32$ GeV, $\Gamma = 0.105$ GeV, $R = 4.4$ GeV^{-1}). The slope and the amplitude of the background were free parameters.

We tested the sensitivity of the fitted number of A_2 events as a function of the fixed A_2 parameters by independently varying the mass, width, and R parameters by one standard deviation. The resultant change in the A_2 events was of the order of 2%, which is small compared to the minimum statistical error of 8%.

The differential cross section was then calculated from the fitted number of A_2 events, $N(t')$, with $1.2 < M(K_S^0K^-) < 1.4$ GeV in each t' interval, by

$$\frac{d\sigma}{dt'}=\frac{KN(t')}{\rho LN_0N_\pi A(t')\Delta t'}\ ,$$

where ρLN_0 gives the number of scattering centers in the hydrogen target, N_π is the number of incident beam particles, $A(t')$ is the acceptance of the apparatus over the t' interval ($\Delta t'$), and K is a product of t'-independent systematic-correction factors such as beam contaminations, counter inefficiencies, K_S^0 charged-decay branching ratios, etc. (A complete list of these factors and their errors is given in Table III.) Details of the determination of some of these numbers are given below. Further details may be found in Ref. 13.

Monte Carlo programs were run using the two

TABLE II. Results of fitting the K^0K^- effective-mass spectra with the CERN missing-mass dipole form and a linear background.

Fit no.	$-t'$ [(GeV/c)^2]	Mass interval (GeV)	χ^2	Degrees of freedom	Rejection of fit (standard deviations)	Total events	Fitted background (events)
(1)	All t'	1.1–1.5	205	76	8.0	3346	1256
(2)	0.0–0.20	1.2–1.4	68	37	3.1	1187	245
(3)	0.20–0.29	1.2–1.4	61.5	37	2.6	502	91.7
(4)	>0.29	1.2–1.4	77	37	3.9	956	182.2
(5)	All t'	1.25–1.35	71	17	6.2	1815	352.8

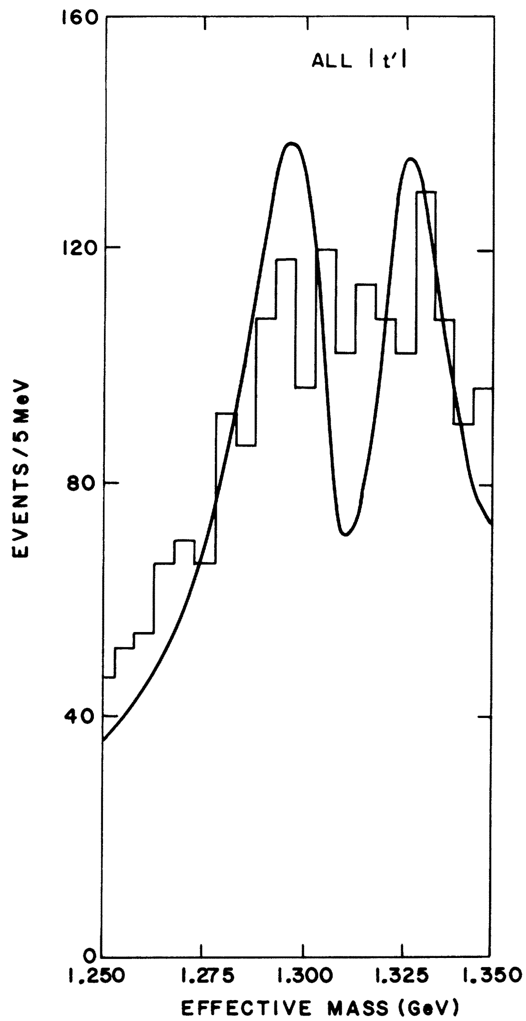

FIG. 9. The $K_S^0K^-$ mass spectrum over all t' for the mass interval $1.25 < M(K_S^0K^-) < 1.35$ GeV. The solid curve is the result of a fit to the spectrum using the dipole form and a linear background where the background level was obtained by a similar fit over the retion $1.1 < M(K_S^0K^-) < 1.5$ GeV (see text).

different momenta (22.4 GeV/c and 23.9 GeV/c). Events of the type

$$\pi^- p \to X^- p, \quad X^- \to K^- K_S^0, \quad K_S^0 \to \pi^+\pi^-$$

were generated as a function of the four kinematic variables, t', M_{X^-}, $\cos\theta$, and ϕ, where M_{X^-} is the effective mass of the resonance, and θ and ϕ are the decay angles of the A_2 as defined in the Gottfried-Jackson frame.[12] These events were followed through the apparatus to determine what fraction of events would survive and be detected. Figs. 10(a) and 10(b) show the observed θ and ϕ distributions corrected by the calculated acceptance. The solid curves on Figs. 10(a) and 10(b) are the results of a maximum-liklihood fit with the form $A\sin^2\theta\cos^2\theta\sin^2\phi$ plus an isotropic term. The fitted level of the isotropic term is $\lesssim 10\%$. The acceptance was then integrated over M_{X^-}, θ, and ϕ (weighted according to a $\sin^2\theta\cos^2\theta\sin^2\phi$ decay distribution as observed above) to yield the acceptance as a function of t' alone. The resulting acceptance is shown in Fig. 11 and is a smooth function of t'.

The average acceptance was 5.19% at 22.4 GeV/c ans 5.39% at 23.9 GeV/c. We estimate a 10% systematic error on the overall acceptance. We note that of the generated events, 78% were eliminated because the K_S^0 decayed either in the target or downstream of the first spark chamber. The acceptance for those events that survive the decay-volume cut is $\approx 25\%$.

We required that the missing mass for a good $K_S^0K^-$ event fall between 0.7 and 1.1 GeV. In order to evaluate the corrections due to this cut, we fitted the recoil missing-mass spectrum in the region $0.6 < MM < 1.18$ GeV to a Gaussian plus a linear background. Then, on the basis of the above fit, we applied a $(3\pm1)\%$ correction to the cross sections for lost events that were associated with recoiling protons that lie outside the selected missing-mass interval. Similarly, we applied a $(3\pm3)\%$ correction for extra events due to "contamination" of the proton peak.

In order to estimate the program's efficiency in detecting A_2^- events, we adopted the following procedure: As each $K_S^0K^-$ event was found, the coordinates of the sparks associated with the π^+, π^-, and K^- for this event were stored in a table. For each event after the first, these sparks were removed from the data and replaced by the stored sparks from the previous event. Then these data were reanalyzed to see if the program could find the previous event with the background associated with the current event. The major losses were due to merging tracks, especially in the upstream arm of the spectrometer, and to confusion in combining two-dimensional views into three-dimensional tracks. The correction factors due to the program efficiencies are given in Table III.

The overall trigger efficiency of our spectrometer on A_2 events is the product of the trigger efficiencies for (a) the scintillator A [$(92\pm2)\%$], (b) the proportional wire chamber [$(98\pm2)\%$], and (c) the $H4$ scintillation-counter hodoscope [$(91.8\pm3)\%$ and $(83.3\pm3)\%$ for the 22.4- and 23.9-GeV/c runs, respectively]. We note that the loss in scintillator A was due to the Landau fluctuations of the energy loss of particles traversing the

TABLE III. Systematic corrections to the cross-section data and the corresponding errors for the reaction $\pi^- p \to A_2^- p$, $A_2^- \to K_S^0 K^-$ at 22.4 and 23.9 GeV/c.

	$P = 22.4$ GeV/c	$P = 23.9$ GeV/c
Proton cut	1.03 ±0.01	1.03 ±0.01
Contamination of recoil-proton peak	0.97 ±0.03	0.96 ±0.04
Program efficiency	1.20 ±0.11	1.32 ±0.13
Trigger efficiency	1.21 ±0.06	1.33 ±0.07
Beam-system efficiency	1.022	1.022
Losses in the data-handling system	1.008	1.022
Empty-target correction	0.984 ±0.013	0.984 ±0.013
e^- and μ^- beam contamination	1.036 ±0.005	1.034 ±0.005
Nuclear attenuation in the target	1.036 ±0.01	1.036 ±0.01
K^0K^- interactions in the target	1.05 ±0.01	1.05 ±0.01
Pion decay in spectrometer [a]	1.03 ±0.01	1.03 ±0.01
Events lost for $-t' > 1.0$ (GeV/c)^2 [b]	1.02 ±0.01	1.02 ±0.01
$K^0 \to K_S^0$ branching ratio	2.0	2.0
$K_S^0 \to \pi^+\pi^-$ branching ratio	1.452	1.452

[a] The decay of K^- in our spectrometer is included in the acceptance correction.
[b] Correction applied to total cross section, not differential cross section.

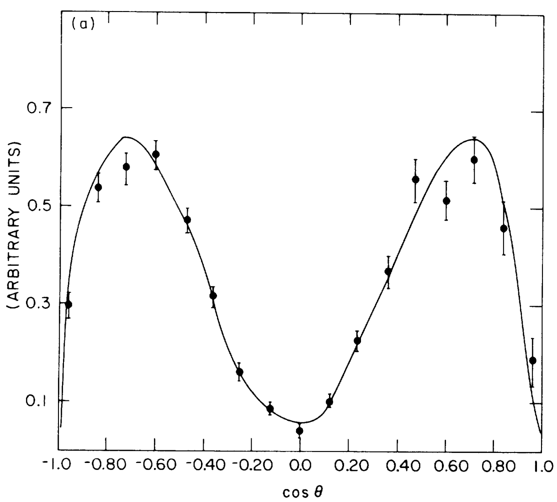

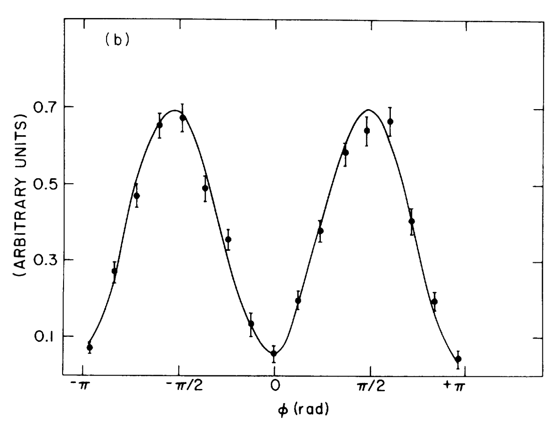

FIG. 10. Decay angular distributions (corrected for acceptance) as a function of Gottfried-Jackson variables, (a) $\cos\theta$ and (b) ϕ. The solid lines on (a) and (b) are the results of maximum-likelihood fits to the form $A\cos^2\theta\sin^2\theta\sin^2\phi$ plus an isotropic background.

counter. Eight percent of the true single-particle events had pulse heights above the two-particle threshold and thus were vetoed. We have neglected the contribution to the overall trigger efficiency from scintillation-counter hodoscope $H4'$, since the individual counters in $H4'$ were virtually 100% efficient. Since the above trigger inefficiencies were uncorrelated, we combined the errors in quadrature. The resultant trigger efficiencies of the apparatus for A_2 events were $(82.8 \pm 4.1)\%$ and $(75.1 \pm 4.1)\%$ for the 22.4- and 23.9-GeV/c runs, respectively.

There are three dominant systematic uncertainties: (1) the acceptance (10%), (2) the program efficiency (8%), and (3) the trigger efficiency (5%). Since these effects are uncorrelated, we combined these uncertainties and the others listed in Table III in quadrature. The resultant systematic error is 14%.

We present the differential-cross-section data in Tables IV and V and Figs. 12(a) and 12(b).

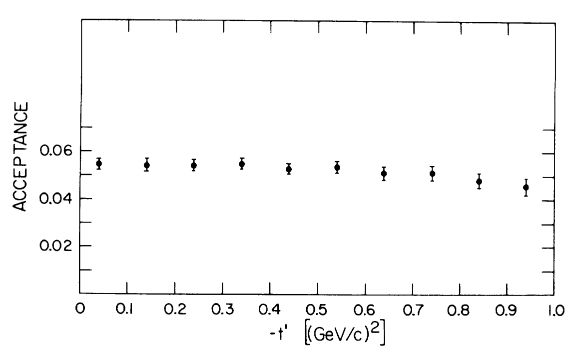

FIG. 11. The acceptance of the spectrometer for $1.2 < M(K_S^0 K^-) < 1.4$ GeV as a function of t' at 23.9 GeV/c.

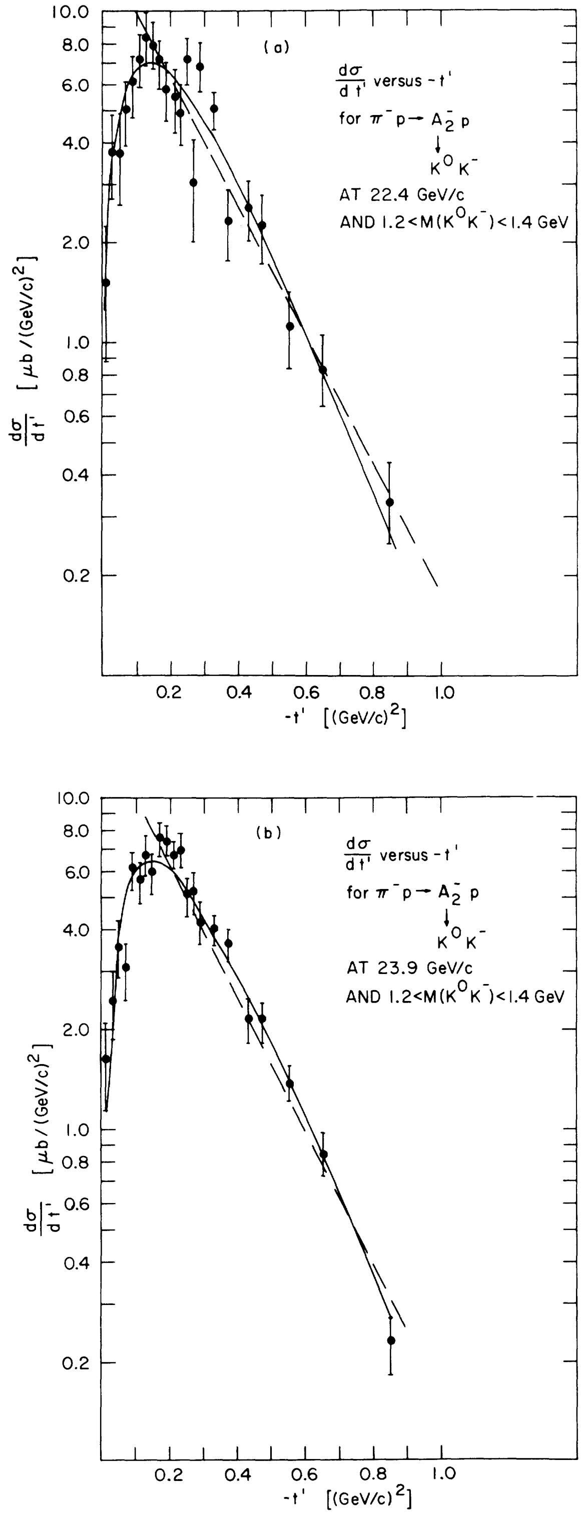

FIG. 12. $d\sigma/dt$ for the reaction $\pi^- p \to A_2^- p$, $A_2^- \to K^0 K^-$ versus $-t'$ for $1.2 < M(K_S^0 K^-) < 1.4$ GeV. The solid curve is the result of a fit to the form $At'e^{bt'}$. The dashed curve is the result of a fit to the form $Ae^{bt'}$ for $|t'| > 0.13$ (GeV/c)^2. (a) 22.4 GeV/c and (b) 23.9 GeV/c.

Tables IV and V also give the fitted number of A_2 events and the acceptance as a function of t' at each momentum. The errors indicated are statistical only. There is an additional 14% rms systematic error.

The differential cross sections show a forward dip[14] for $|t'| < 0.1$ (GeV/c)^2 and an exponential fall approximately as $e^{4.5t'}$ for $|t'| > 0.13$ (GeV/c)^2. We fitted the differential-cross-section data for $0.0 < |t'| < 1.0$ (GeV/c)^2 with a form $A(-t')^a e^{bt'}$. The results of the fit gave a value for the parameter a consistent with 1 [i.e., $a = 0.94 \pm 0.14$ (GeV/c)$^{-2}$ and $a = 1.2 \pm 0.11$ (GeV/c)$^{-2}$ for the 22.4 and 23.9 GeV/c runs, respectively]. We then fitted the data with the form $At'e^{bt'}$ for $0.0 < |t'| < 1.0$ (GeV/c)^2 giving the values $b = 7.25 \pm 0.26$ and 7.01 ± 0.14 (GeV/c)$^{-2}$ for the 22.4- and 23.9-GeV/c runs, respectively.

These results are tabulated in Table VI and are shown as the solid ($At'e^{bt'}$) and dashed ($Ae^{bt'}$) curves on Fig. 12. The errors on the parameters shown in Table VI are statistical only.

The total cross sections for the reaction

$$\pi^- p \to A_2^- p, \quad A_2^- \to K^0 K^-$$

at 22.4 and 23.9 GeV/c are 2.64 ± 0.10 μb and 2.51 ± 0.07 μb, respectively. The errors on the cross sections are statistical only; there is also a 14% rms systematic error. These cross sections were calculated for the mass interval of the $K_S^0 K^-$ between 1.2 and 1.4 GeV and have been extrapolated in t' to cover the whole forward peak.

In order to compare our total cross sections to those obtained for the $\rho^0\pi^-$ decay mode as given in Ref. 15, we have divided them by the branching ratio

$$\frac{A_2^- \to K^0 K^-}{A_2^- \to \rho^0 \pi^-} = 0.13,$$

as derived from the Particle Data Group tables.[16] In addition, we have multiplied our data by a factor of 0.95[17] to allow for the fact that we have not separated the natural- and unnatural-parity exchange contributions. Our results are shown as the open squares in Fig. 13, and are in good agreement with the curve fit to the $\rho^0\pi^-$ data. Much of the earlier apparent disagreement[9] between our previous K^0K^- experiment[5] (shown as the open triangle in Fig. 13) and the $\rho^0\pi^-$ data that existed at that time had already been removed by a combination of new data from Serpukhov[15] for the reaction $\pi^- p \to \rho^0 \pi^- p$ at 25 GeV/c which tends to lower the fitted curve, and a new[16] value for the $K^0K^-/\rho^0\pi^-$ branching ratio.

TABLE IV. Fitted events, acceptance, and differential cross section as functions of $-t'$ for the reaction $\pi^- p \to A_2^- p$, $A_2^- \to K^0 K^-$ at 22.4 GeV/c and $1.2 < M(K^0K^-) < 1.4$ GeV. Errors shown are statistical only. There is also a 14% rms overall systematic error.

$-t'$ [(GeV/c)^2]	Fitted events	Acceptance	$\frac{d\sigma}{dt'}\left[\frac{\mu b}{(GeV/c)^2}\right]$
0.0–0.02	7.8	0.054 ±0.001	1.55 ±0.74
0.02–0.04	19.0	0.054 ±0.001	3.77 ±1.01
0.04–0.06	18.7	0.054 ±0.001	3.72 ±1.13
0.06–0.08	25.4	0.054 ±0.001	5.04 ±1.13
0.08–0.10	30.9	0.054 ±0.001	6.14 ±1.23
0.10–0.12	36.4	0.054 ±0.001	7.23 ±1.25
0.12–0.14	42.6	0.054 ±0.001	8.47 ±1.45
0.14–0.16	40.1	0.054 ±0.001	7.97 ±1.29
0.16–0.18	35.9	0.054 ±0.001	7.14 ±1.23
0.18–0.20	28.8	0.053 ±0.001	5.83 ±1.19
0.20–0.22	27.6	0.053 ±0.001	5.59 ±1.15
0.22–0.24	24.2	0.053 ±0.001	4.90 ±1.05
0.24–0.26	35.9	0.053 ±0.001	7.27 ±1.28
0.26–0.28	14.8	0.052 ±0.001	3.06 ±1.05
0.28–0.30	33.0	0.052 ±0.001	6.81 ±1.17
0.30–0.35	60.9	0.052 ±0.001	5.02 ±0.64
0.35–0.40	27.4	0.051 ±0.001	2.31 ±0.51
0.40–0.45	29.6	0.050 ±0.002	2.54 ±0.46
0.45–0.50	26.0	0.049 ±0.002	2.28 ±0.45
0.50–0.60	25.6	0.048 ±0.002	1.14 ±0.26
0.60–0.70	17.8	0.046 ±0.002	0.83 ±0.20
0.70–1.0	19.3	0.042 ±0.003	0.33 ±0.08

TABLE V. Fitted events, acceptance, and differential cross section functions of $-t'$ for the reaction $\pi^- p \to A_2^- p$, $A_2^- \to K^0 K^-$ at 23.9 GeV/c and $1.2 < M(K^0K^-) < 1.4$ GeV. Errors shown are statistical only. There is also a 14% rms overall systematic error.

$-t'$ [(GeV/c)^2]	Fitted events	Acceptance	$\frac{d\sigma}{dt'}\left[\frac{\mu b}{(GeV/c)^2}\right]$
0.0–0.2	19.2	0.055 ±0.001	1.64 ±0.48
0.02–0.04	28.6	0.055 ±0.001	2.44 ±0.58
0.04–0.06	41.3	0.055 ±0.001	3.51 ±0.62
0.06–0.08	36.3	0.055 ±0.001	3.09 ±0.62
0.08–0.10	72.8	0.055 ±0.001	6.20 ±0.75
0.10–0.12	66.4	0.055 ±0.001	5.65 ±0.75
0.12–0.14	80.2	0.055 ±0.001	6.83 ±0.83
0.14–0.16	70.3	0.055 ±0.001	5.98 ±0.76
0.16–0.18	88.9	0.055 ±0.001	7.57 ±0.83
0.18–0.20	87.2	0.055 ±0.001	7.43 ±0.80
0.20–0.22	79.3	0.055 ±0.001	6.76 ±0.80
0.22–0.24	79.9	0.054 ±0.001	6.93 ±0.78
0.24–0.26	59.0	0.054 ±0.001	5.12 ±0.69
0.26–0.28	60.2	0.054 ±0.001	5.22 ±0.71
0.28–0.30	48.8	0.054 ±0.001	4.23 ±0.66
0.30–0.35	116.6	0.054 ±0.001	4.05 ±0.39
0.35–0.40	103.2	0.053 ±0.001	3.65 ±0.39
0.40–0.45	60.9	0.053 ±0.002	2.15 ±0.28
0.45–0.50	61.2	0.053 ±0.002	2.16 ±0.28
0.50–0.60	77.3	0.053 ±0.002	1.37 ±0.16
0.60–0.70	46.0	0.051 ±0.002	0.85 ±0.13
0.70–1.0	33.9	0.047 ±0.003	0.23 ±0.04

VI. SUMMARY AND CONCLUSIONS

A. A_2 mass spectrum

From the reaction $\pi^- p \to K_S^0 K^- p$ at ≈ 23 GeV/c, we have analyzed 3346 events in the effective-mass range $1.1 < M(K_S^0 K^-) < 1.5$ GeV and the t' range $0.0 < |t'| < 1.0$ (GeV/c)^2. The spectrum summed over all t' is well fitted by a single D-wave Breit-Wigner form. No two-peak structure is observed and the previously reported CERN MMS dipole-type fit is rejected by 8 standard deviations. We then narrowed the mass region to $1.25 < M(K_S^0 K^-) < 1.35$ GeV to concentrate on the reported dip and found a rejection by 6σ.

When the data are divided into t' regions of $|t'| < 0.2$, $0.2 < |t'| < 0.29$, and $|t'| > 0.29$ (GeV/c)^2, each spectrum is again well fitted by a single D-wave Breit-Wigner form. The best-fit values of M_0, Γ_0 and R for each of these spectra are consistent with each other and with the values obtained for the overall fit (see Table I). The CERN dipole form (even with the mass range restricted to $1.2 < M(A_2) < 1.4$ GeV) is unlikely in each of the above t' regions by 3.1σ, 2.6σ, and 3.9σ, respectively.

Thus our data are completely consistent with a single Breit-Wigner shape that is independent of t'. We find no evidence for any anomalous structure. The CERN dipole form is completely rejected for the overall spectrum and has a probability of less than 1% in any t' subsample studied.

In addition to our data, (1) experiments[7,8] sim-

TABLE VI. Fits to the differential cross sections.

Functional form of $d\sigma/dt'$	P (GeV/c)	t' region [(GeV/c)^2]	Fit parameters [(GeV/c)$^{-2}$]
$At'e^{bt'}$	22.4	$0.0 < \|t'\| < 1.0$	$b = 7.25 \pm 0.26$
$At'e^{bt'}$	23.9	$0.0 < \|t'\| < 1.0$	$b = 7.01 \pm 0.14$
$Ae^{bt'}$	22.4	$0.13 < \|t'\|$	$b = 4.47 \pm 0.25$
$Ae^{bt'}$	23.9	$0.13 < \|t'\|$	$b = 4.59 \pm 0.15$

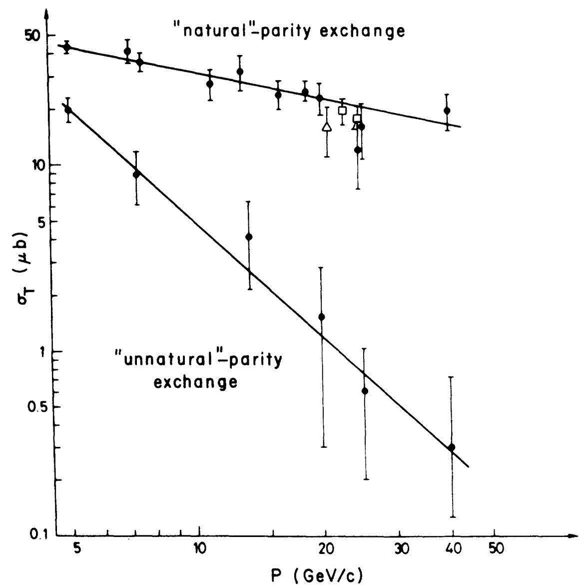

FIG. 13. A plot of the available data on the reaction $\pi^-p \to A_2^-p$, $A_2^- \to \rho^0\pi^-$ above 3.9 GeV/c and including our data on the reaction $\pi^-p \to A_2^-p$, $A_2^- \to K^0K^-$, adjusted by the $A_2 \to \rho^0\pi^-/A_2 \to K^0K^-$ (= 7.7) branching ratio. The solid points and the fit lines are taken from Ref. 14. The open triangle represents $K_S^0K^-$ data from our previous experiment,[5] and the open squares represent data from this experiment. All K^0K^- cross sections have been multiplied by 0.95 to allow for the fact that we have not separated the natural- and unnatural-parity-exchange contributions.

ilar to those done with the CERN MMS and CBS contradict the original results, (2) reanalyses[18] of the original experiments have resulted in the reduction of the original claim of 6–7 standard deviations to a 3–4 standard-deviation dip in the range $0.21 < t < 0.29$ (GeV/c)^2, and (3) a recent experiment[19] on the mode $A_2 \to \eta\pi$ in the t region $0.27 < |t| < 0.42$ (GeV/c)^2 yields no evidence for a split A_2. The weight of the evidence leads us to conclude that the A_2 is a single unsplit D-wave Breit-Wigner resonance.

B. Differential cross sections

The differential cross sections exhibit a forward dip for $|t'| < 0.1$ (GeV/c)^2. The data are well fitted over the region $0.0 < |t'| < 1.0$ by the form $At'e^{bt'}$ with $b \approx 7.0$ (GeV/c)$^{-2}$ (see Table VI).

C. Total cross sections

The total cross sections for the reaction $\pi^-p \to A_2^-p$, $A_2^- \to K^0K^-$ were determined from the differential cross sections for $1.2 < M(A_2) < 1.4$ GeV. We find

$$\sigma = 2.6 \pm 0.4\ \mu\text{b at } 22.4\ \text{GeV}/c\ ,$$

$$\sigma = 2.5 \pm 0.4\ \mu\text{b at } 23.9\ \text{GeV}/c\ ,$$

where the above includes a 14% systematic error.

We have compared these cross sections to those obtained in the $A_2 \to \rho^0\pi^-$ mode by using the $(A_2^- \to \rho^0\pi^-)/(A_2^- \to K^0K^-)$ branching ratio, and we have found good agreement.

ACKNOWLEDGMENTS

The authors wish to thank the members of the AGS and EP & S Divisions of the Accelerator Department of Brookhaven National Laboratory for their help in the execution of this experiment. We thank our group technicians, M. Conforte, G. Leigh, T. Mogavero, A. Roesch, and R. Wheeler, for their extended and valuable efforts in the construction and operation of the spectrometer and D. Bartolomeo, L. Davis, A. Friedman, J. Gould, R. Imossi, and C. Zein for their efficient and cooperative operation of the BNL On-Line Data Facility. We also thank W. Miller and S. Eiseman, who were instrumental in the design and construction of the electronics for the proportional wire chambers, and U. Mallik, who provided valuable assistance during the operation and analysis of this experiment.

*Now at Rutgers University.
†Work supported by the National Science Foundation.
‡Work performed under the auspices of the Energy Research and Development Administration.

[1]B. Levrat, C. A. Tolstrup, P. Schübelin, C. Nef, M. Martin, D. C. Maglić, W. Kienzle, M. N. Focacci, L. Dubal, and G. Chikovani, Phys. Lett. 22, 714 (1966); G.Chikovani, M. N. Focacci, W. Kienzle, C. Lechanoine, B. Levrat, B. Maglić, M. Martin, P. Schübelin, L. Dubal, M. Fischer, P. Grieder, H. A. Neal, and C. Nef, *ibid.* 25B, 44 (1967).

[2]H. Benz, G. E. Chikovani, G. Damgaard, M. N. Focacci, W. Kienzle, C.Lechanoine, M. Martin, C. Nef, P. Schübelin, R. Baud, B. Bošnjaković, J. Cotteron, R. Klanner, and A. Weitsch, Phys. Lett. 28B, 233 (1968).

[3]R. Baud, H. Benz, B. Bošnjaković, D. R. Botterill, G. Dangaard, M. N. Focacci, W. Kienzle, R. Klanner, C. Lechanoine, M. Martin, C. Nef, V. Roinishvili, P. Schübelin, A. Weitsch, H. Blumenfeld, H. Jöstlein, and P. Lecomte, Phys. Lett. 31B, 397 (1970).

[4]M. Alston-Garnjost, A. Barbaro-Galtieri, W. F. Buhl, S. E. Derenzo, L. D. Epperson, S. M. Flatté, J. H. Friedman, G. R. Lynch, R. L. Ott, S. D. Protopopescu, M. S. Rabin, and F. T. Solmitz, Phys. Lett. 33B, 607

(1970).

[5]K. J. Foley, W. A. Love, S. Ozaki, E. D. Platner, A. C. Saulys, E. H. Willen, and S. J. Lindenbaum, Phys. Rev. Lett. 26, 413 (1971); Phys. Rev. D 6, 747 (1972).

[6]G. Grayer, B. Hyams, C. Jones, P. Schlein, W. Blum, H. Dietl, W. Koch, H. Lippmann, E. Lorenz, G. Lütjens, W. Männer, J. Meissburger, U. Stierlin, and P. Weilhammer, Phys. Lett. 34B, 333 (1971).

[7]D. Bowen, D. Earles, W. Faissler, D. Garelick, M. Gettner, M. Glaubman, B. Gottschalk, G. Lutz, J. Moromisato, E. I. Shibata, Y. W. Tang, E. von Goeler, H. R. Blieden, G. Finocchiaro, J. Kirz, and R. Thun, Phys. Rev. Lett. 26, 1663 (1971); C. M. Ankenbrandt, B. B. Brabson, R. R. Crittenden, R. M. Heinz, J. C. Krider, J. E. Mott, H. A. Neal, and A. J. Pawlicki, *ibid.* 29, 1688 (1972).

[8]D. M. Binnie, L. Camilleri, A. Duane, A. R. Faruqi, D. A. Garbutt, W. G. Jones, M. E. Kay, M. Lewis, P. J. Nicholson, I. Siotis, P. N. Upadhyay, J. C. Wilson, I. F. Burton, S. G. Frank, R. George, M. Haque, and J. C. McEwen, Phys. Lett. 36B, 257 (1971).

[9]C. Michael, in *Proceedings of the XVI International Conference on High Energy Physics, Chicago-Batavia, Ill., 1972,* edited by J. D. Jackson and A. Roberts (NAL, Batavia, Ill., 1973), Vol. 3, p. 165.

[10]Reported by V. Chaloupka, in *Proceedings of the XVII International Conference on High Energy Physics, London, 1974,* edited by J. R. Smith (Rutherford Laboratory, Chilton, Didcot, Berkshire, England, 1974), pp. II-22, II-24.

[11]A more detailed technical description of the apparatus is given by K. J. Foley, W. A. Love, S. Ozaki, E. D. Platner, A. C. Saulys, E. H. Willen, and S. J. Lindenbaum, Nucl. Instrum. Methods 108, 33 (1973).

[12]J. D. Jackson, Nuovo Cimento 34, 1644 (1964).

[13]M. Margulies, doctoral thesis, The City University of New York, 1975 (unpublished).

[14]The forward dip is characteristic of resonance production via the exchange of particles with natural spin-parity. Such exchange does not populate the $m = 0$ substate, which is the only one allowed for 0° production.

[15]Y. M. Antipov, G. Ascoli, R. Busnello, M. N. Kienzle-Focacci, W. Kienzle, R. Klanner, A. A. Lebedev, P. Lecompte, V. Rainishvili, A. Weistsch, and F. A. Yotch, Nucl. Phys. B63, 153 (1973).

[16]Particle Data Group, Phys. Lett. 50B, 1 (1974).

[17]The factor of 0.95 is based on the observed ratio of the natural to total cross sections for the $\rho\pi$ mode at ~20 GeV as derived from Fig. 13.

[18]R. E. Diebold, in *Proceedings of the XVI International Conference on High Energy Physics, Chicago-Batavia, Ill., 1972,* edited by J. D. Jackson and A. Roberts (NAL, Batavia, Ill., 1973), Vol. 3, p. 1.

[19]A. W. Key, G. Conforto, M. A. Kramer, D. G. Underwood, R. M. Mobley, R. Prepost, D. H. Tompkins, and M. S. Witherell, Phys. Rev. Lett. 30, 503 (1973); D. Underwood, G. Conforto, M. A. Kramer, A. W. Key, R. M. Mobley, R. Prepost, D. H. Tompkins, and M. S. Witherell, Phys. Rev. D 11, 2345 (1975).